

Your access to this publication is provided through the subscription of Korea University.

Applied Physics Letters / Volume 97 / Issue 25 / ORGANIC ELECTRONICS AND PHOTONICS

[Previous Article](#) | [Next Article](#)

Appl. Phys. Lett. 97, 253309 (2010); doi:10.1063/1.3530448 (3 pages)

The vertically stacked organic sensor-transistor on a flexible substrate

FULL-TEXT OPTIONS: FREE

Read Online (HTML)
 Download PDF
 Permissions / Reprints

Shin Woo Jeong¹, Jin Wook Jeong¹, Seongpil Chang¹, Seung Youl Kang², Kyoung Ik Cho², and Byeong Kwon Ju¹

¹Display and Nanosystem Laboratory, College of Engineering, Korea University, Anam-dong, Seongbuk-Gu, Seoul 136-713, Republic of Korea

²Convergence Components and Materials Research Laboratory, Electronics and Telecommunications Research Institute, Gajeong-Ro, Yuseong-Gu, Daejeon 138, Republic of Korea

(Received 10 September 2010; accepted 3 December 2010; published online 23 December 2010)

- Abstract
- References (22)
- Article Objects (4)
- Related Content

Alerts Tools Share

The authors report on the photo-response characteristics of flexible sensor-transistor circuits (ST-circuits) made with (poly(3-hexylethiophene)/phenyl-C₆₁-butyric acid methyl ester) (P3HT/PCBM) bulk heterojunction polymer and pentacene-based organic field-effect transistors, which are stacked via poly(dimethylsiloxane) (PDMS) on the plastic substrate. The results indicate that the anode-source current is variable because of both the charge separation of the photogenerated excitons and the accumulated charges at the OFET channel layer. The light dependent photo response ($\Delta I/I_0$) is modulated from 0.47 to 1.9 by the gate-source voltage at the fixed anode-source voltage of the ST-circuits.

KEYWORDS and PACS

Keywords

conducting polymers, excitons, field effect transistor circuits, flexible electronics, integrated optoelectronics, optical sensors, organic field effect transistors, organic semiconductors, photoconductivity, semiconductor heterojunctions


PACS

85.60.-q
Optoelectronic devices

85.30.Tv
Field effect devices

Google calendar

ADVERTISEMENT



Ground loops
hard to find?
Find them fast
with the
Loop Slooth
without
disconnecting
anything!

CONFERENCE ORGANIZERS:

Enjoy fast,
cost-effective
publication of
your meeting's
key research!

AIP

The vertically stacked organic sensor-transistor on a flexible substrate

Shin Woo Jeong,¹ Jin Wook Jeong,¹ Seongpil Chang,¹ Seung Youl Kang,² Kyoung Ik Cho,² and Byeong Kwon Ju^{1,a)}

¹Display and Nanosystem Laboratory, College of Engineering, Korea University, Anam-dong, Seongbuk-Gu, Seoul 136-713, Republic of Korea

²Convergence Components and Materials Research Laboratory, Electronics and Telecommunications Research Institute, Gajeong-Ro, Yuseong-Gu, Daejeon 138, Republic of Korea

(Received 10 September 2010; accepted 3 December 2010; published online 23 December 2010)

The authors report on the photo-response characteristics of flexible sensor-transistor circuits (ST-circuits) made with (poly(3-hexylethiophene)/phenyl-C₆₁-butyric acid methyl ester) (P3HT/PCBM) bulk heterojunction polymer and pentacene-based organic field-effect transistors, which are stacked via poly(dimethylsiloxane) (PDMS) on the plastic substrate. The results indicate that the anode-source current is variable because of both the charge separation of the photogenerated excitons and the accumulated charges at the OFET channel layer. The light dependent photo response ($\Delta I/I_0$) is modulated from 0.47 to 1.9 by the gate-source voltage at the fixed anode-source voltage of the ST-circuits. © 2010 American Institute of Physics. [doi:10.1063/1.3530448]

The industrial demand for the flexible, low-cost, lightweight, low-temperature fabrication of electronics has led to much progress in organic electronics, such as organic light-emitting diodes (OLEDs) and radio-frequency identification cards, because the organic materials can be fabricated on a flexible substrate.^{1,2} In addition, integrated organic sensors using organic field-effect transistors (OFETs) to detect chemical analytes,^{3,4} pressures,^{5,6} temperatures,⁷ and light⁸ have a great potential to increase their performance or to include various functions for display and sensor applications. Therefore, integrated organic optoelectronics using OFETs are an alternative candidate for flexible sensor systems⁹ compared to devices based on inorganic materials.^{10,11} However, the integration of organic photosensor (OPS) and organic driving circuits, such as an active matrix backplane on the same plane, can cause an unstable performance when they are exposed to light because the active layer of an OFET is also sensitive to the incident light.¹² Moreover, the integration of organic devices requires a passivation process using insulators, such as a thick polymer, in order to prevent unexpected dissolution damage caused by organic solvents.^{13,14} To address this, vertically isolated layers in the stacked configuration of the devices, especially for the organic optical devices made using different materials, create solvent and light-barriers at the same time for large integration.

In this paper, we use a soft elastomer that serves simultaneously as a scratch protector and for compatibility compensation for the plastic substrate. This device configuration enables vertical stacking. Figure 1(a) shows the materials and device structure of the OPS/OFET. The aluminum cathode of the OPS is used as a light-barrier to prevent photoactivation of the pentacene layer from incident light. And, the variable photoresponse is possible by both the reduced dark current from conductive element of OPS [shown in Fig. 1(b)] through the series resistance of OFET at a fixed voltage and the variable resistance of it. Therefore, this device has advantages to demonstrate not only the flexible integrated opto-

electronics but also the controllable photodetecting systems.

We used [poly(3-hexylethiophene)/phenyl-C₆₁-butyric acid methyl ester] (P3HT/PCBM) (purchased from Nano-C, Westwood, MA) that is based on the composites of an electron-donating conjugated polymer and an electron-accepting fullerene.^{15,16} The OPS is processed on indium tin oxide (ITO) patterned (by photolithography) 125 μm thin poly(ethylene terephthalate) (PET) substrates. The sheet resistance is 20 Ω/sq ; the film thickness is 150 nm. The (Poly(3,4-ethylenedioxythiophene) poly(styrenesulfonate)) (PEDOT:PSS) (Bayer, Leverkusen, Germany) layer was deposited by spin-coating at 2500 rpm and annealed at 120 °C for 10 min. The P3HT:PCBM (1: 0.8) solution in chlorobenzene at 22 mg/ml was prepared. The 90 nm of aluminum was deposited by thermal evaporation. Then, it is annealed at 150 °C for 10 min. In order to integrate the OPS device and OFET onto the same substrate, about 1 mm of poly(dimethylsiloxane) (PDMS) [Dow Corning, Sylgard 184 (Seoul)] was prepared. The etching process was omitted because the contact pads are made by the patterned membrane. For the OFET fabrication, a 140 nm thick Au was evaporated onto the PDMS. The chemical compatibility of the PDMS to the organic materials and its adhesion to Au as a functional interlayer have been proved in an earlier report.¹⁷ The 750 nm thick poly-4-vinylphenol was spin coated and annealed at 200 °C for 10 min. In spite of the low PEN glass tempera-

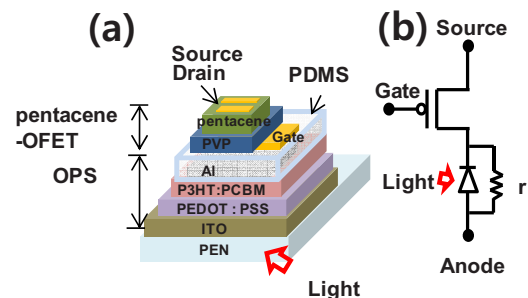


FIG. 1. (Color online) (a) The schematic illustration of the vertically stacked sensor-transistor circuit. (b) The equivalent circuit diagram of the fabricated devices. The resistive element of the OPS is connected in parallel.

^{a)}Author to whom correspondence should be addressed. Tel.: +82-2-3290-3237. FAX: +82-2-921-1325. Electronic mail: bkju@korea.ac.kr.

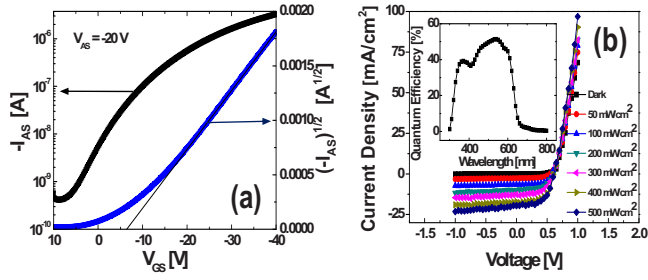


FIG. 2. (Color online) (a) The transfer curves of the sensor-transistor circuits under no illumination in air. (b) The current density-voltage (J - V) characteristics of the organic photosensor devices. The inset is the curve of the measured EQE of the separated organic photosensor devices.

ture, we can align each layer using optical microscopy. The 70 nm pentacene layer was evaporated using a thermal evaporation system (DOV Co., Ltd., Seoul) at room temperature. The 100 nm thick Au source and drain electrodes (W/L: 500/100 μm) were evaporated in the same chamber. Finally, the two devices were integrated onto the same substrate. The OPSs have active areas of 9 mm^2 . The electrical characteristics were measured using a Keithley model 2400 and a semiconductor parameter analyzer (Keithley 4200 SCS). The class-A sola simulator with a 150 W xenon lamp [Newport (California)] adjusted using a NREL-calibrated mono-Si solar cell, with a KG-2 filter, for an approximately AM 1.5 G1 sun light intensity is used. The external quantum efficiency (EQE) was measured using incident photo-to-current conversion equipment [PV Measurements Inc. (Colorado)]. The calibration was performed using a silicon photodiode G425, which is NIST-calibrated as a standard.

In Fig. 2(a), the integrated device is turned on by applying a negative V_{GS} . We note that the anode to source voltage is $V_{AS} = V_{OPS} + V_{DS}$ of the OFET, which is the aim of this investigation into the interlocking characteristics of the integrated OPS and OFET. The field-effect mobility of the OPS connected to the OFET is calculated to be 0.24 $\text{cm}^2/\text{V s}$ by using $I_{AS} = (WC_i/2L)\mu_{\text{sat}}(V_{GS} - V_{\text{th}})^2$ where I_{AS} is the anode-source current, C_i is the capacitance per unit area, V_{th} is the threshold voltage, and V_{GS} is the gate to source voltage. The calculated current on/off ratio was 8190 at $V_{AS} = -20$ V. The threshold voltage of -6.5 V was defined by the extrapolation of the I_{AS} versus V_{GS} curve. In Fig. 2(b), the current-voltage (I - V) characteristics of the fabricated OPS under an illumination in air show that the trend of the light intensity is coincident with the current density of the OPS devices. Although the performance of our device is lower than previously reported ones,^{18,19} this device shows a sufficient performance to transfer the photocurrent to the pentacene-based OFET. The inset of Fig. 2(b) shows the EQE spectra for the OPS separated from the OFET. The EQE maximum is about 50% at the wavelength of 550 nm.

The experimental data for the analysis in terms of V_{GS} dependence are presented in Fig. 3. The I_{AS} of the sensing ST-circuit is measured on the basis of a fixed voltage, that is, a fixed V_{AS} (-0.3 V) and a V_{GS} from -5 to -30 V. The light exposure is triggered to start with each gate reverse bias step and lasts about 10 s. The I_{AS} increases according to the increased light intensity when the reverse gate bias increases. We found that the dark current of the separated OPS, -0.5 mA at -0.3 V [shown in Fig. 2(b)], is reduced to -17 nA at $V_{GS} = -5$ V. This result originates from the fact that the low-

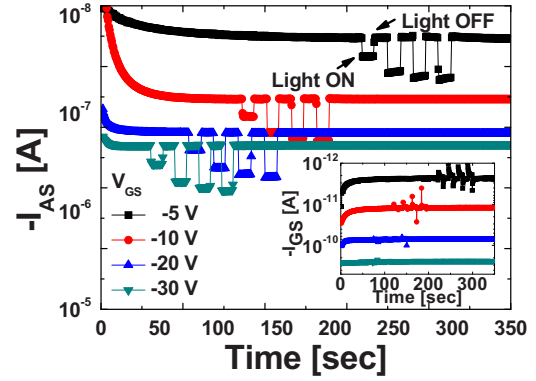


FIG. 3. (Color online) The change in the I_{AS} as a function of time when the sensor-transistor is exposed to cycles of exposure to light intensities ranging from 50 to 500 mW/cm^2 in air. The given V_{AS} is -0.3 V. The inset shows the change in the I_{GS} at the same time when the response current is measured.

ered voltage distribution to OPS induced decreased dark current because the series resistance of the OPS is only about 600 Ω as compared with the calculated total series resistance, which is varied from 17.6 to 1.42 $\text{M}\Omega$ at fixed $V_{AS} = -0.3$ V.

On the other hand, the transient time to steady-state is shortened as the gate reverse bias is increased. We believe that it is attributed to the swift movement of the mobile hole carriers by the increased electric field at the channel layer so that the degree of accumulation and stabilization quickly reaches its saturation point according to the gate-voltage dependent carrier mobility $\mu_{\text{lin}} = (L/WV_{AS}C_i)(\partial I_{AS}/\partial V_{GS})$ in the linear regime.²⁰ This is matched to the slope of the I_{AS} versus time, which is dependent on V_{GS} . In addition, the simultaneously measured I_{GS} is sufficiently low with appreciable variations occurring only in the overshooting phase because the order of the I_{GS} value is negligible in comparison to the order of the on current value. (Fig. 3, inset) So, we conclude that the pentacene layer in the fabricated device is not activated by the light exposure, and the electrical sensing operation of the ST-circuits is largely dependent on the light intensity.

In Fig. 4, the response current $\Delta I = I_{\text{photo}} - I_{\text{dark}}$ is plotted against the irradiated light intensity for each V_{GS} . The calculated photoresponse $P = (I_{\text{photo}} - I_{\text{dark}})/I_{\text{dark}}$ from Figs. 3 and 4 changed from 0.47 to 1.9. The photoresponse increases as the V_{GS} increased while the photoinduced current from the OPS

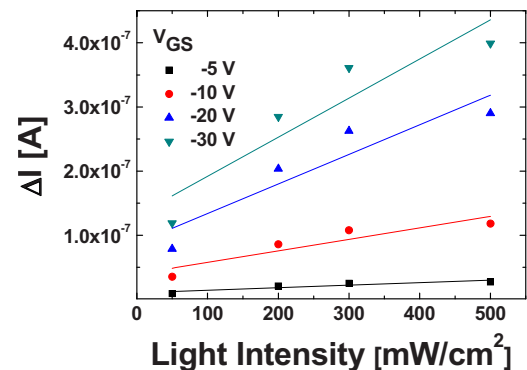


FIG. 4. (Color online) The response characteristics for the sensor-transistor circuit dependent on the V_{GS} vs different light intensities at a fixed $V_{AS} = -0.3$ V.

is constant. It means that the current variation in the output current of the ST-circuit is modulated by the gate-voltage dependent channel resistance of the OFET, when the V_{AS} is fixed. But, the response range of $R = \Delta I_{\max} / \Delta I_{\min} = (I_{\max} - I_{\text{dark}}) / (I_{\min} - I_{\text{dark}})$ for each V_{GS} condition from -5 to -30 V shows 2.96, 3.33, 3.68, and 3.35, respectively, where I_{\max} is the on state current at 500 mW/cm^2 , I_{dark} is the dark current, and I_{\min} is the on state current at 50 mW/cm^2 . The decreased response range at $V_{GS} = -30$ V is resulted from the current reduction by prolonged negative gate biasing at high V_{GS} , which allows the charge trapping near the channel.²¹ And the linear fit of ΔI versus light intensity in Fig. 4 shows deviation at the point of light intensity, 500 mW/cm^2 . The gradually decreasing gradient of the response current to the light intensity is attributed to the operation of the OFET, which limits the photocurrent of the OPS at high light intensities. In principle, when the total voltage across the circuit is fixed, the OFET can be saturated for a large photocurrent and the voltage bias on the OPS is diminished.²²

In summary, the vertically integrated OPS and OFET using a PDMS elastomer showed variable gate dependent photoresponse at fixed low V_{AS} . The photoresponse ($\Delta I/I_0$) is modulated from 0.47 up to 1.9 by both the V_{GS} and light at a fixed I_{AS} of -0.3 V. Therefore, our device offers a simpler route for device integration and tunable optical properties. In addition, this stacked configuration is beneficial for integration into the innovative concept of flexible optoelectronics, such as smart OLEDs or integrated portable detection systems in *point-of-care* diagnostics.

This work was supported by the IT R&D Program (Grant No. 2008-F-024-02, Development of Mobile Flexible Input/Output Platform) of MKE in Korea, Basic Science Research Program through the National Research Foundation of Korea (NRF) funded by the Ministry of Education, Science and Technology (No. 2009-0083126) and the International Research and Development Program of the National Research Foundation of Korea (NRF) funded by the Ministry of

Education, Science and Technology (MEST) of Korea (Grant No. D00048).

- ¹S. R. Forrest, *Nature (London)* **428**, 911 (2004).
- ²E. Cantatore, T. C. T. Geuns, G. H. Gelinck, E. van Veenendaal, A. F. A. Gruijthuisen, L. Schrijnemakers, S. Drews, and D. M. de Leeuw, *IEEE J. SSC.* **42**, 1 (2007).
- ³P. Svensson, D. Nilsson, R. Forchheimer, and M. Berggren, *Appl. Phys. Lett.* **93**, 203301 (2008).
- ⁴B. K. Crone, A. Dodabalapur, A. Gelperin, L. Torsi, H. E. Katz, A. J. Lovinger, and Z. Bao, *Appl. Phys. Lett.* **78**, 2229 (2001).
- ⁵T. Someya, T. Sekitani, S. Iba, Y. Kato, H. Kawaguchi, and T. Sakurai, *Proc. Natl. Acad. Sci. U.S.A.* **101**, 9966 (2004).
- ⁶Y. Chao, W. Lai, C. Chen, H. Meng, H. Zan, and S. Horng, *Appl. Phys. Lett.* **95**, 253306 (2009).
- ⁷T. Someya, Y. Kato, T. Sekitani, S. Iba, Y. Noguchi, Y. Murase, H. Kawaguchi, and T. Sakurai, *Proc. Natl. Acad. Sci. U.S.A.* **102**, 12321 (2005).
- ⁸T. D. Anthopoulos, *Appl. Phys. Lett.* **91**, 113513 (2007).
- ⁹L. Zhou, A. Wanga, S. C. Wu, and J. Sun, *Appl. Phys. Lett.* **88**, 083502 (2006).
- ¹⁰T. N. Ng, W. S. Wong, M. L. Chabinye, S. Sambandan, and R. A. Street, *Appl. Phys. Lett.* **92**, 213303 (2008).
- ¹¹M. Zirkl, A. Haase, A. Fian, H. Schon, C. Sommer, G. Jakopic, G. Leising, B. Stadlober, I. Graz, N. Gaar, R. Schwodiauer, S. Bauer-Gogonea, and S. Bauer, *Adv. Mater.* **19**, 2241 (2007).
- ¹²Y.-Y. Noh, D.-Y. Kim, Y. Yoshida, K. Yase, B.-J. Jung, E. Lim, and H.-K. Shim, *Appl. Phys. Lett.* **86**, 043501 (2005).
- ¹³S. M. Seo, C. Baek, and H. H. Lee, *Adv. Mater.* **20**, 1994 (2008).
- ¹⁴T. Someya, Y. Kato, S. Iba, Y. Noguchi, T. Sekitani, H. Kawaguchi, and T. Sakurai, *IEEE Trans. Electron Devices* **52**, 2502 (2005).
- ¹⁵J. Y. Kim, K. Lee, N. E. Coates, D. Moses, T. Q. Nguyen, M. Dante, and A. J. Heeger, *Science* **317**, 222 (2007).
- ¹⁶G. Li, V. Shrotriya, J. Huang, Y. Yao, T. Moriarty, K. Emery, and Y. Yang, *Nature Mater.* **4**, 864 (2005).
- ¹⁷Y. L. Loo, T. Someya, K. W. Baldwin, Z. Bao, P. H. A. Dodabalapur, H. E. Katz, and J. A. Rogers, *Proc. Natl. Acad. Sci. U.S.A.* **99**, 10252 (2002).
- ¹⁸T. Yamanari, T. Taima, K. Hara, and K. Saito, *Sol. Energy Mater. Sol. Cells* **93**, 759 (2009).
- ¹⁹Y. Kim, S. A. Choulis, J. Nelson, and D. D. C. Bradley, *Appl. Phys. Lett.* **86**, 063502 (2005).
- ²⁰P. V. Necliudov, M. S. Shur, D. J. Gundlach, and T. N. Jackson, *J. Appl. Phys.* **88**, 6594 (2000).
- ²¹A. Salleo and R. A. Street, *J. Appl. Phys.* **94**, 471 (2003).
- ²²C. Kyle Renshaw, X. Xu, and S. R. Forrest, *Org. Electron.* **11**, 175 (2010).